CHAPTER 2

Synthesis and Characterisation of Low Band-Gap Copolymers Based on BODIPY Derivatives and Fabrication of OPVS

2.1 ABSTRACT

A series of four soluble BODIPY derivatives bearing EDOT and EDTT units have been synthesised *via* Stille coupling. The influence of these units, as well as the difference of leaving the core open (open-BODIPY) or closing the BODIPY ring by a N-B-N bridge, have been studied in detail by cyclic voltammetry and UV-vis absorption spectroscopy. Due to the ease of electropolymerisation of EDOT and EDTT, the four monomers were subjected to electropolymerisation. The electronic properties of these polymers were studied by cyclic voltammetry.

Different chemical polymerisations (Sugimoto, nitrosonium mediated polymerisation, Yamamoto polymerisation and Stille coupling polymerisation) were studied in order to prepare copolymers bearing bis-EDTT units and the BODIPY core along the conjugated backbone. Additionally, a co-polymer based on bis-EDOT units and the BODIPY core was also synthesised *via* Stille coupling polymerisation.

The polymers obtained *via* Stille coupling **p(BDP-bisEDOT)** and **p(BDP-bisEDTT)**) were fully characterised and their photovoltaic properties were investigated. Power conversion efficiencies of 0.95 and 0.46% were measured for **p(BDP-bisEDOT)** and **p(BDP-bisEDTT)**, respectively.

2.2. SYNTHESIS

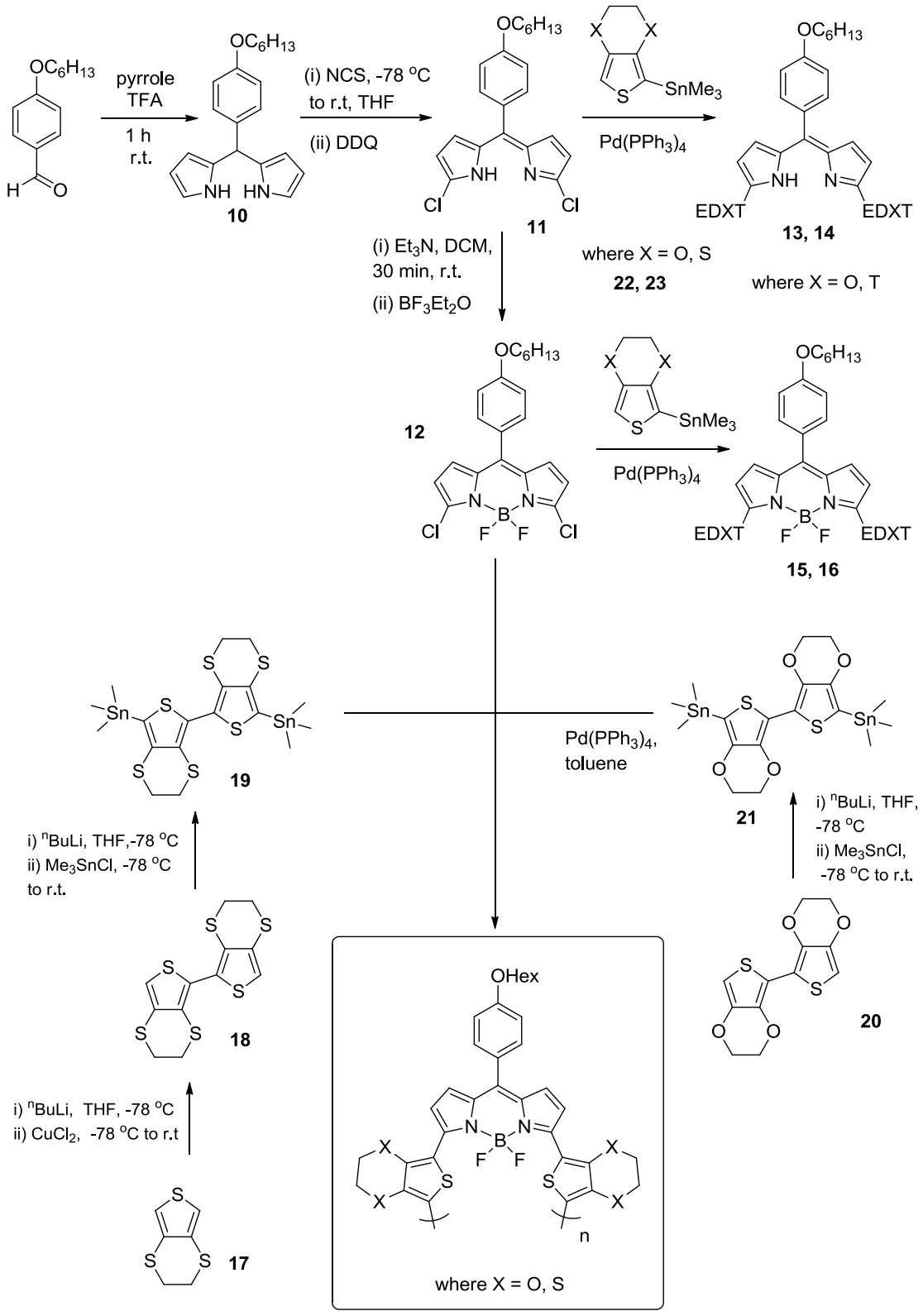

2.3. INTRODUCTION

In the last two decades, derivatives of the 4,4-difluoro-4-bora-3*a*,4*a*-diaza-*s*-indacene dye, better known as BODIPY (**24**), have attracted great interest among researchers due to its outstanding fluorescence properties.[1,2,3] They present high UV-visible absorptions ($\lambda \geq$ 500 nm), sharp fluorescence peaks with high quantum yields (ϕ_f), negligible triplet state formation, and fluorescence lifetimes (τ_f) in the nanosecond range. As a consequence of the small formation of the triplet state, due to a poor intersystem crossing rate (*ca.* 10^6 s^{-1}) of most of the BODIPY derivatives, the degradation of these compounds *via* self-produced singlet oxygen is low.[4] Furthermore, the relatively short synthetic routes to obtain them, the ease of tuning properties by multiple substitutions of the core, chemical robustness, good solubilities and thermal stability make BODIPYs interesting candidates to be used in materials chemistry. Consequently, BODIPYs have been used for different applications such as electroluminescent devices,[5] electrogenerated chemiluminescence,[6,7] laser dyes,[8,9] chemosensors,[1] labelling reagents,[1] mechanical rotors,[10] molecular logic gates,[11] and solar cells.[12,13,14]

Since the first BODIPY dye was synthesised in 1968 by Treibs and Kreuzer,[15] a vast number of derivatives have been prepared, but the BODIPY core **24** has not been obtained till recently.[16] The rigid BODIPY core has been compared to indacene **25**, the all carbon analogue, and it has been seen as a half unit of a porphyrin macrocyle **26**. As the BODIPY core is usually highly substituted, for convenience figure 1 explains the numbering. Positions 3 and 5 are also referred to as *alpha* positions (α), 2 and 6 as *beta* (β) and position 8 as *meso*; they will be used as nomenclature in this chapter.

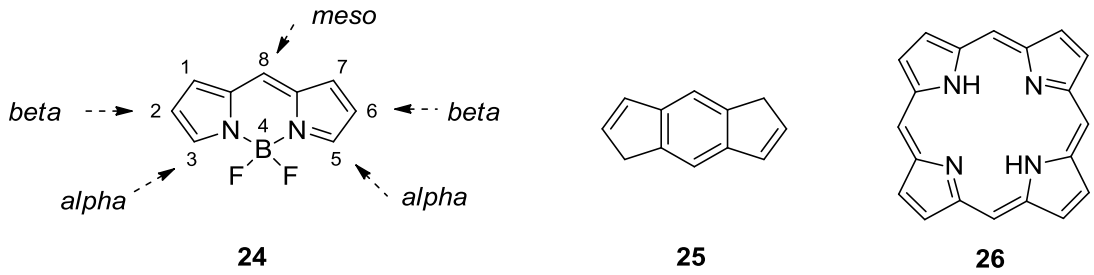

24 **25** **26**

Figure 2.1. Chemical structure of BODIPY (**24**), indacene (**25**) and porphyrin (**26**)

The synthesis of BODIPYs has been mainly achieved by acid catalysed condensation of pyrrole and/or its derivatives with highly electrophilic carbonyl compounds such as acyl chlorides or aldehydes to link the two pyrrole rings by a methene bridge. In the first case, subsequent deprotonation by an amine and addition of boron trifluoride diethyl etherate yields the BODIPY core directly. Condensation with aldehydes leads to unstable dipyrromethanes[17] (**27**) that have to be oxidised with 2,3-dichloro-5,6-dicyano-*p*-benzoquinone (DDQ) or 2,3,5,6-tetrachloro-*p*-benzoquinone (*p*-chloranil) to obtain a dipyrromethene. Subsequent, treatment with an amine and boron trifluoride diethyl etherate leads to BODIPYs. Although the majority of the BODIPYs in the literature are substituted, aromatic aldehydes can also react with pyrrole to obtain unsubstituted BODIPYs. In this case the condensation step is carried out by using high excess of pyrrole, which also plays the role of solvent, to avoid polycondensations that derive in the formation of polymers.

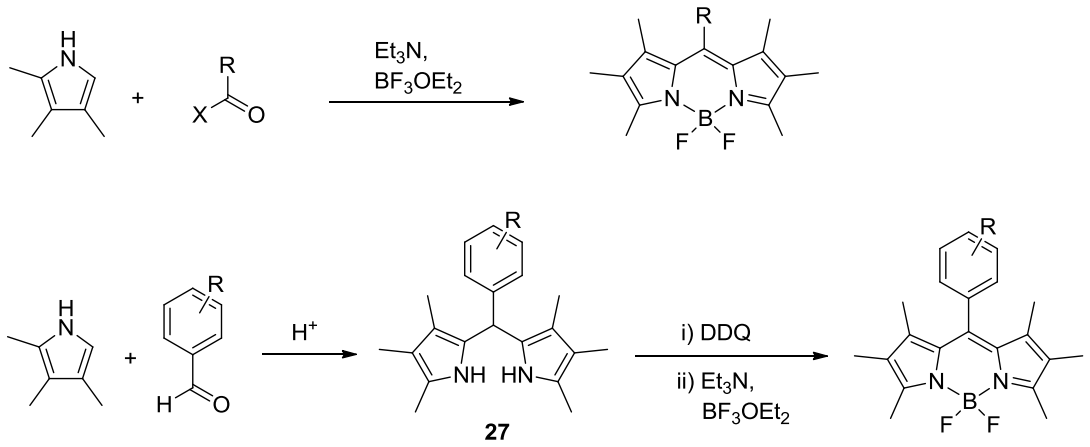

Scheme 2.1. Different routes to synthesise BODIPY derivatives (X = Cl)

Whereas following these two reaction pathways symmetrical BODIPYs are obtained, unsymmetrical BODIPYs can be obtained by condensation of a carbonyl-containing pyrrole derivative with another pyrrole (that is not substituted at the 2-position) by using acids or phosphoryl chloride. By all these synthetic pathways, and with relatively easy purification methods (usually column chromatography and precipitations are required), BODIPYs can be obtained in a multi-gram scale.

The chemical robustness of the core gives the opportunity to carry out further derivatisation and therefore tune it finely to obtain the desired properties. The *meso*-position has been mainly substituted with substituted aromatic rings (phenyl). Although the aromatic ring on the *meso*-positions does not have a major effect on the electronic properties, as it usually sits orthogonal to the BODIPY core, bulky substituents on the ring can avoid stacking and therefore an increase in the fluorescence quantum yield can be achieved. Substituents on the phenyl ring have also been incorporated to chelate analytes and be used in sensors by switching on + off the fluorescence of the BODIPYs in the presence or absence of the analyte.[1,2]

Starting from 2,4–dimethyl-pyrrole, unsubstituted BODIPYs on the *beta*-positions can be obtained (**28**). These two positions can undergo electrophilic substitution reactions. Different electrophiles such as chlorosulfonic acid (to obtain water-soluble derivatives) or bromine (or iodine in the presence of HIO_3) have been used. The

halogenated derivatives can also be obtained using either *N*-bromosuccinimide, *N*-iodosuccinimide or *N*-chlorosuccinimide.

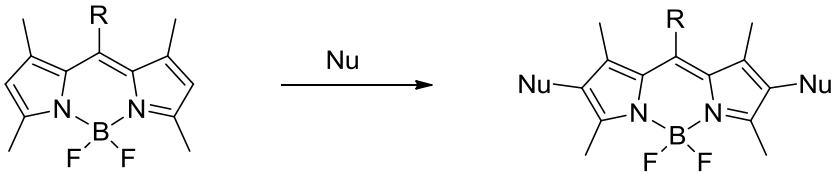

28

Scheme 2.2. Reaction of BODIPYs with nucleophiles species

Although a direct method to obtain *alpha*-substituted BODIPY derivatives is by reacting pyrrole derivatives bearing the desired substituents, sometimes this approach is not feasible. The completely unsubstituted BODIPY can be directly functionalised by oxidative nucleophilic substitution of hydrogen (ONSH) at the *alpha*-positions.[18] Reaction of the unsubstituted BODIPY with a nucleophile (nitrogen, sulfur, carbon or oxygen centred nucleophiles) followed by treatment with oxygen yields 3-monosubstituted or 3- and 5-disubstituted BODIPYs. The methyl groups on the *alpha*-positions of **28** are relatively acidic and after deprotonation under mild conditions, they can react with electron rich aromatic aldehydes to give a Knoevenagel-type reaction.[19] The extension of the conjugation of the BODIPY core in these systems is enlarged by introducing the styryl groups and marked bathochromic shifts in the absorption and fluorescence are observed.[20]

Chlorination of the *alpha*-positions is a very useful way of obtaining 3- and 5-substituted BODIPYs. The fact that the 3- and 5-positions are electron-deficient makes chlorinated derivatives susceptible to nucleophilic aromatic substitution.[21] Therefore, chlorine atoms can be either mono- or di-substituted by nucleophiles such as alkoxides, amines and thiolalkoxides.

Although the extension of conjugation can also be achieved by the fusion of benzene rings to the pyrrole rings, such synthetic strategies are usually more complicated.[1] An important way of increasing the conjugation beyond that of the BODIPY core is by

introducing aryl units at the alpha positions. The chlorine atoms on these positions can also react *via* metal-catalysed cross-coupling reactions, and Stille, Suzuki-Miyaura, Heck and Sonogashira cross-coupling reactions can proceed with yields of around 50-68% for both mono- and di-substituted BODIPY cores.[22] Similarly, another interesting synthetic approach combines the last two modifications. The *alpha*-chlorinated derivative is first substituted by a thioalkyl groups and subsequently it reacts with an electron-rich aryl-tin derivative *via* Liebeskind-Srogl coupling.[23] This methodology can be of special interest when the BODIPY bears more halogenated atoms, as the coupling with the thioalkyl groups is chemoselective over aryl bromides.[24]

Although the vast majority of the synthesised BODIPY derivatives are single molecules, the versatility of the core has led to its incorporation into higher macrostructures such as nanoparticles,[25] dendrimers[26] and polymers, along the main chain[27] or as pendant groups.[28,29] By replacing the two fluorine atoms of the core with akynyl derivatives,[2] followed by Sonogashira-Hagihara cross-coupling type reaction with di-acetylenyl functionalised aromatic rings, highly fluorescent self-assembled polymers were obtained.[27] Following a similar approach, the BODIPY core was also copolymerised with quinolate units *via* Sonogashira coupling.[30] Even if in both cases the BODIPY core is in the polymer backbone and conjugated systems are incorporated, the conjugation is not extended along the polymer (it can be deduced from the UV-visible absorption spectra), as the co-monomers show independent behaviour.

Likewise, the BODIPY core has also been incorporated into conjugated polymers. The majority of the conjugated polymers published so far contain a 1-, 3-, 5- and 7-tetramethyl-substituted BODIPY core (see Scheme 2.2). The halogenation of the *beta*-positions of the core enables different types of polymerisations to be completed, such as cross-coupling reactions. In these kinds of polymers, high conjugation is usually desired as it can lead to considerable bathochromic shifts both in the absorption and emission spectra. However, the extension of conjugation can be hindered by the presence of the four methyl groups and the comonomers, mainly

aromatic rings, would lie out of the plane. A lower degree of conjugation is then expected and the bathochromic shifts diminished. The main strategy to overcome this problem is to incorporate two ethynylene groups to the core. The 2- and 6-diiodinated core reacts first with ethynyltrimethylsilane *via* Sonogashira coupling, which is then deprotonated with tetrabutylammonium fluoride. The resulting derivative (**29**) can be polymerised with the previously diiodinated core or copolymerised with other diiodinated aromatic rings *via* Sonogashira coupling to achieve deep-red emissive polymers.[31,32] The same procedure was used to synthesise donor-acceptor conjugated copolymers bearing BODIPY units and organic thin film transistors were fabricated.[33] Depending on the acceptor unit, the copolymers showed *p*- or *n*-type semiconducting behaviour. Whereas most of the conjugated polymers are hydrophobic due to the presence of long aliphatic chains, by following the aforementioned approach and by incorporating multiple oligo(ethylene glycol)methyl ether side chains both on the BODIPY and on the comonomers, highly water-soluble and near infrared emissive conjugated polymers have been obtained.[34]

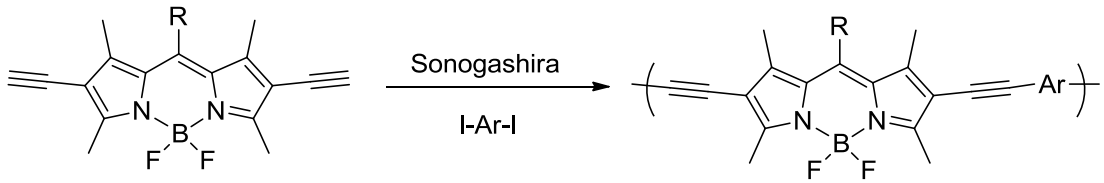

29

Scheme 2.3. Polymerisation of Bodipys through the *beta* positions.

Cihaner and Algi have also incorporated the BODIPY into conjugated polymers by electropolymerisation. A di-thienylpyrrole unit bearing a BODIPY derivative attached to the N atoms of the pyrrole rings was first electropolymerised.[35] The BODIPY was also incorporated into the main polymeric backbone by coupling a 2- and 6-dibrominated BODIPY derivative with 2-(trimethylstannyl)-thiophene and subsequent electropolymerisation.[36] By incorporating the EDOT units into the polymer ambipolar behaviour was observed. The electrochromic properties of all three polymers were investigated in these studies.[37]

Although the BODIPY core has been used in solar cells (a further discussion will be carried in chapter 4), to the best of my knowledge there is only one study where the BODIPY core has been incorporated into conjugated polymers and tested as donors in bulk heterojunction type organic photovoltaics.[14] Polymers **30** and **31** were synthesised following the approach previously described. The two low band gap copolymers showed high absorption in the near infrared. The best reported power conversion efficiencies are 1.2 and 2.0 % for **30** and **31**, respectively.

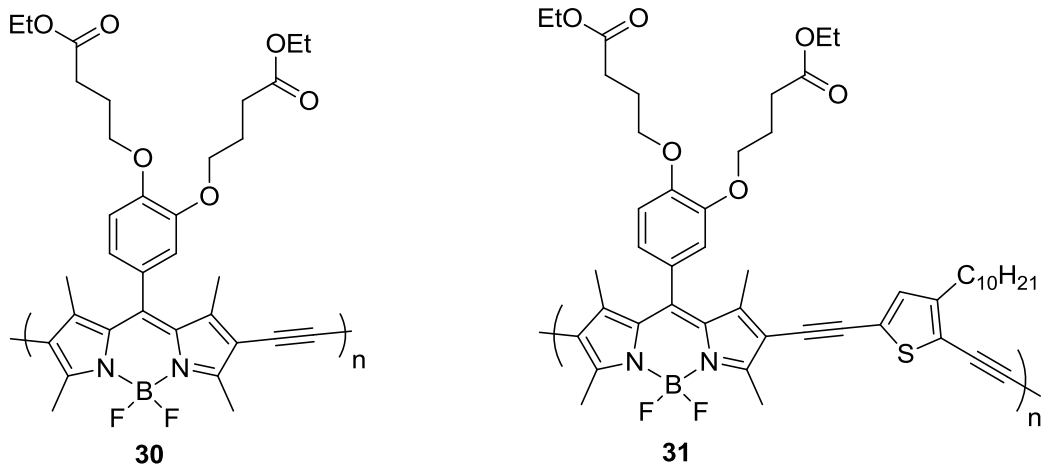

Figure 2.2. Bodipy polymers used in OPVs

2.4 SYNTHESIS OF MONOMERS 13-16

This project aims to incorporate the BODIPY structure into the main polymeric chain. Whereas, the majority of the BODIPY containing polymers have been linked through the *beta* positions, this project focuses on producing conjugated polymers through the *alpha*-positions. In previous work carried out in Prof. P.J. Skabara's group, a BODIPY core was incorporated into a conjugated polymer by electrochemical polymerisation of a BODIPY core disubstituted with two EDOT units on the *alpha*-positions.[38] The redox properties of the polymer were investigated by cyclic voltammetry and a low band gap polymer was obtained (0.8 eV). The polymer showed also good reversibility upon oxidation and reduction.

With the aim of chemically synthesising BODIPY containing copolymers for organic photovoltaic applications, a suitable BODIPY derivative was chosen. Highly soluble conjugated polymers are desirable for the fabrication of solar cells (techniques such as drop-casting are usually utilised). Therefore, an aromatic aldehyde with a long alkoxyl chain on the *para* position was used to prepare the BODIPY derivative.

Scheme 2.4 shows the synthetic route to obtain the BODIPY derivative that was used for copolymerisation. The synthetic route was initiated by condensation of the *para*-substituted benzaldehyde with a high excess of pyrrole (it also acts as solvent) and in the presence of catalytic amounts of trifluoroacetic acid (TFA), to yield a yellow dipyrromethane oil. The high excess of pyrrole that is used in this reaction prevents compound **9** from undergoing further condensation that would lead to the formation of undesired polycondensed systems. Compound **10** can be isolated by column chromatography or by high vacuum distillation. Several attempts were also carried out to synthesise the same dipyrromethane in water by using HCl, but low conversion was observed.[39] Even though mechanical stirring was used, the low solubility in water of the long aliphatic chain of the benzaldehyde inhibited the reaction significantly.

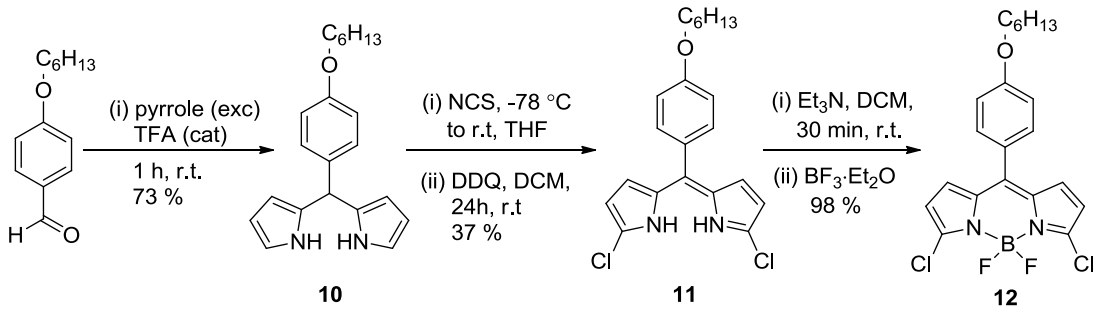

Scheme 2.4. Synthesis of the BODIPY core **12**.

Compound **10** was chlorinated on the two available *alpha*-positions of the pyrrole rings following a known procedure.[40] The resultant dichlorinated intermediate was used without purification and immediately oxidised with DDQ to give dipyrromethene (**11**). This oxidation step provides an extension of the π-conjugated

system by linking the two aromatic heterocycles through a methylene bridge. Compound **11** was first deprotonated with triethylamine and reacted with $BF_3 \cdot Et_2O$ overnight at room temperature to obtain the BODIPY core (**12**) as a deep red tar. At this stage, special care has to be taken, and even more when the reaction is carried out in high scale, as the evolution of the reaction involves the formation of highly dangerous hydrogen fluoride.

3,4-Ethylenedioxythiophene, EDOT, and its derivatives have been widely used in conjugated polymers. The polymerisation of EDOT, either chemically or electrochemically, yields a highly conductive polymer (PEDOT). Properties such as low redox potentials, moderate band gaps, good stabilities and transparency in the doped states make them attractive building blocks to be used in conjugated polymers.[41]

Following the outstanding results of incorporating additional sulfur atoms and higher chalcogen atoms to the structure of tetrathiafulvalene unit (TTF, see chapter 3), EDOT analogues have been prepared.[42] In that sense, in Skabara's group, 3,4-ethylenediselenathiophene,[43] where oxygen is replaced by selenium atoms, and the all-sulfur analogue of EDOT, 3,4-ethylenedithiathiophene (EDTT) have been investigated showing interesting properties which make them useful building blocks to be used in conjugated copolymers.[44,45] Consequently, the incorporation of EDOT and EDTT on the aforementioned BODIPY structure was investigated.

Four different monomers by a combination of open-ring (they are dipyrromethenes, and not BODIPYs, but for ease of comparison they will be referred to as *open-BODIPYs*) and close-ring BODIPYs with either EDOT or EDTT were synthesised. At this stage of the study, several synthetic routes were investigated in order to make it possible to obtain the best yields. This step was crucial to achieve a high degree of polymerisation when the copolymers were prepared (the synthesis of the polymers is discussed in the next section).

The open-ring BODIPY was first reacted with trimethyl-stannylated-EDTT (**23**) derivative *via* microwave-assisted Stille coupling. Even though microwave-assisted Stille couplings have been reported to be successful for other systems,[46] in this case the reaction yielded only 10% of product, similar to the previously reported value.[38] The coupling was also carried using conventional heating and the yield increased up to 53%, which means a yield higher than 70% per coupling position. For the coupling with trimethyl-stannylated-EDOT (**22**), slightly higher yields were obtained (yield of 12% and 57% in microwave and with conventional heating, respectively).

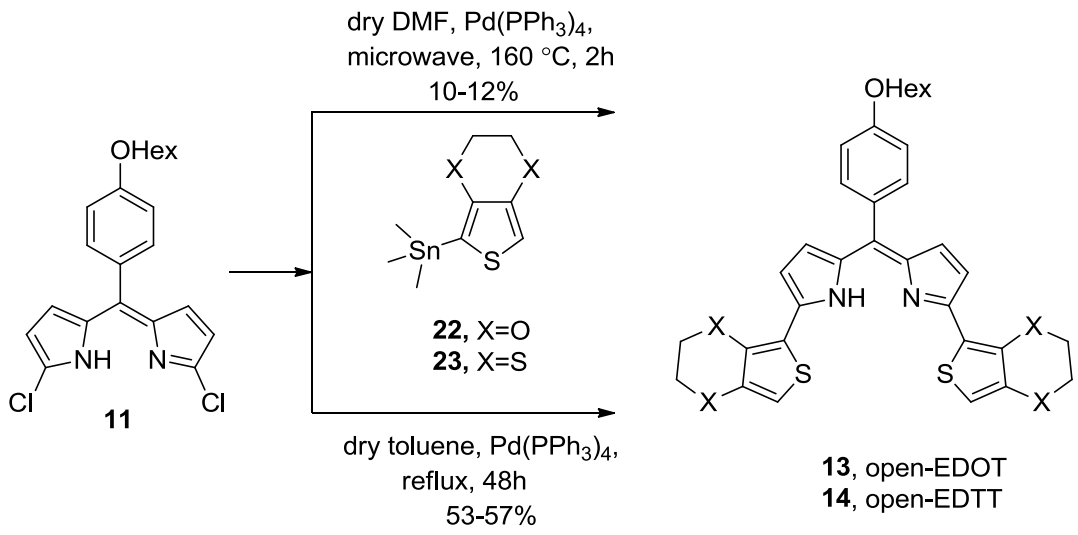

Scheme 2.5. Synthesis of *open-ring BODIPYs*.

The two ring-close BODIPY compounds (**close-EDOT** and **close-EDTT**) were also obtained following two different synthetic routes in order to investigate the best way of obtaining them. The BODIPY with two EDOT units was synthesised from the already substituted open-ring BODIPY. Deprotonation of dipyrromethene (**open-EDOT**) and followed by treatment with boron trifluoride yields compound **close-EDOT** in 60%. This yield is clearly low for the ring closure, as yields over 85% are usually obtained. Thin layer chromatography showed that full conversion of (**open-EDOT)** was not achieved, which may be due to steric hindrance. On the other hand, to obtain compound (**close-EDTT**) the ring was first closed and subsequent cross coupling *via* Stille coupling with conventional heating was carried out.

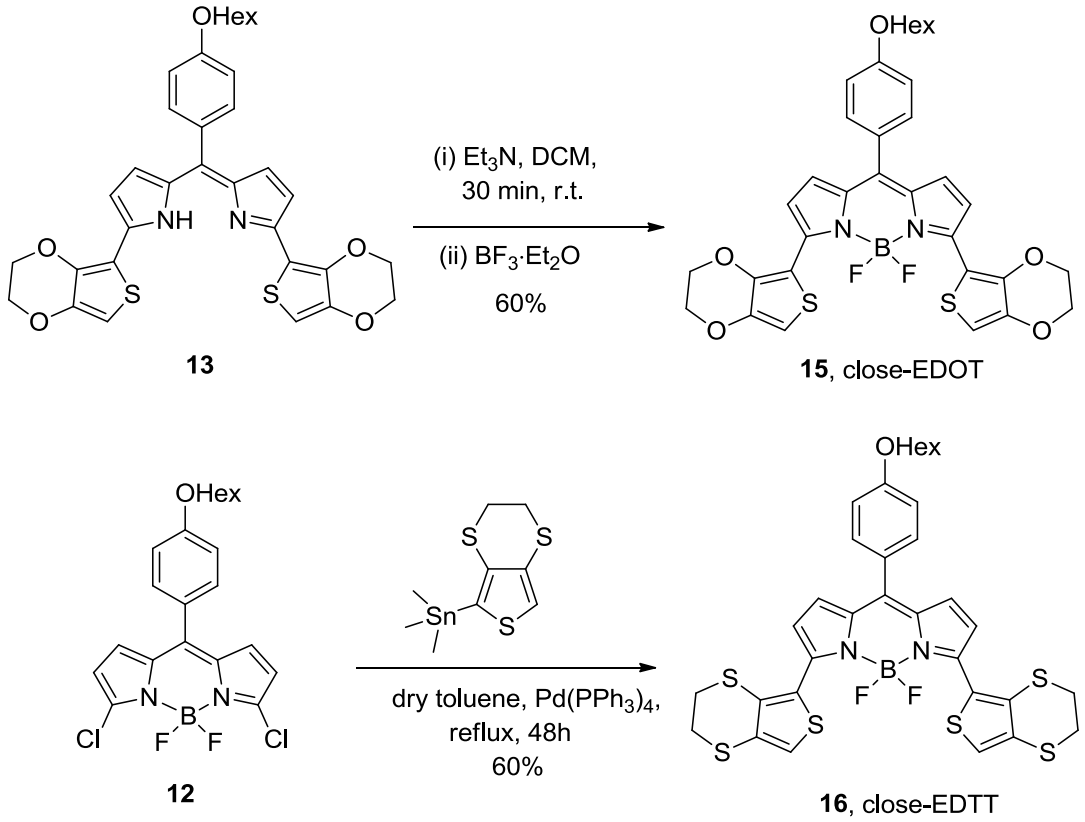

Scheme 2.6. Synthesis of *close-BODIPYs.*

2.5 CHARACTERISATION OF MONOMERS 13-16

2.5.1 UV-Visible Absorption Spectroscopy of Monomers 13-16

The optical properties of the monomers were investigated by UV-visible absorption spectroscopy. Figure 2.3. shows the absorption spectra of the four monomers in dichloromethane solution. The spectra of **11** and **12** have also been included to facilitate the comparison between open and close systems. Table 2.1. summarises the obtained optical data.

The four monomers show intense absorption peaks at wavelengths longer than 558 nm. The maxima for **open-EDOT** and **open-EDTT** are at 558 and 562 nm respectively. The two close ring systems are bathochromically shifted in comparison

with the open ones. The maxima for **close-EDOT** appears at 641nm (it shows a shoulder at 602 nm) and for **close-EDTT** at 614 nm. In comparison with most of the BODIPY systems that present narrow absorption bands at wavelengths ≥ 500 nm (**12** presents a sharp peak at 511 nm), the peaks in the monomers are broad. These transitions can be attributed to the presence of an internal charge transfer process.

Likewise, by comparison of the chlorinated precursors with the monomers a significant bathochromic shift of the peaks can be observed. This is a result of the effective conjugation and the increase of the π-conjugated systems. Optical HOMO-LUMO gaps were calculated from the onset of the longest wavelength absorption peaks and are summarised in Table 2.1.

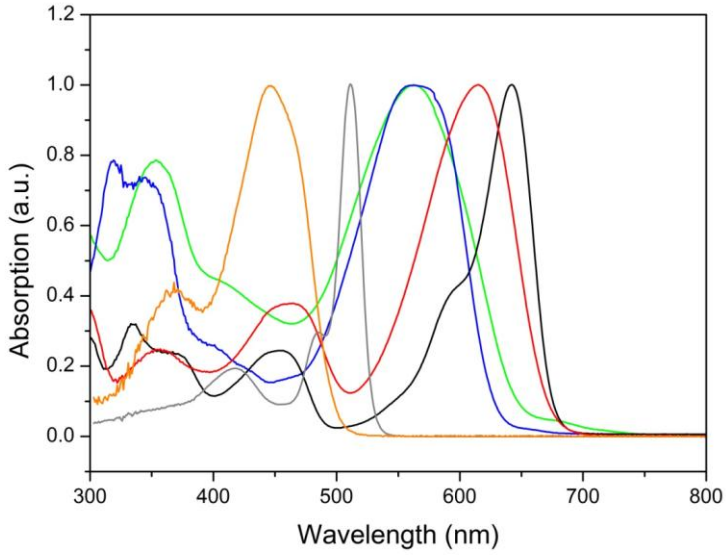

Figure 2.3. Normalised UV-vis absorption spectra (for better comparison) of the *open*- and *close*-*Bodipy* monomers (**13-16**) and **11** and **12**. **Open-EDOT** (blue), **open-EDTT** (green), **close-EDOT** (black), **close-EDTT** (red), **11** (orange) and **12** (grey).

	Absorption peaks / nm	ε / $dm^3mol^{-1}cm^{-1}$	HOMO-LUMO gap / eV
open EDOT	319, 344, 395 (*sh*), 558	61000	1.98
open EDTT	353, 401 (*sh*), 562	82000	1.92
close EDOT	334, 365, 453, 602(*sh*), 641	41000	1.83
close EDTT	356, 462, 614	67500	1.84
11	367, 446	65000	2.48
12	416, 484(*sh*), 511	82500	2.32

Table 2.1. Absorption data and optical HOMO-LUMO gap of *open*- and *close*- *Bodipys* (**13-16**), **11** and **12**.

2.5.2 Electrochemical Properties of Monomers 13-16

The electrochemical behaviour of the previously described four monomers was investigated by cyclic voltammetry. The experiments were carried out in dichloromethane solution, using tetrabutylammonium hexafluorophosphate ($TBAPF_6$) (0.1 M) as the supporting electrolyte. In all cases the monomer concentration was 0.1 mM, the scan rate was 0.1 V/s with *i*R compensation. A glassy carbon, platinum wire and silver wire were used as working electrode, counter electrode and reference electrode, respectively. All the values are quoted *versus* the redox potential of the ferrocene/ferrocenium couple.

The results are shown in Figures 2.4. and 2.5. For convenience and a better understanding, Figure 2.4. shows the oxidation and reduction of the two open BODIPY monomers, whereas the Figure 2.5. shows that of the closed-rings. The oxidation and reduction graphs for each compound were obtained independently and

not as a full cycle, as the presence of irreversible peaks gave imprecise redox behaviours. Likewise, the solutions were bubbled with argon prior to each reduction. Table 2.2. summarises the redox potentials and HOMO and LUMO values of the monomers.

The oxidation of **open-EDOT** and **open-EDTT** show two marked oxidation peaks (Figure 2.4.). The first oxidation in each case occurs at $E_{1/2}$ = +0.24 and +0.26 V for **open-EDOT** and **open-EDTT**, respectively. Both processes are irreversible and are ascribed to the formation of the radical cation species. The second oxidation peaks are due to the formation of the radical dication and they appear at +0.66 and +0.67 V, for **open-EDOT** and **open-EDTT**, respectively. It is worth noting that the electrochemical behaviour of these monomers upon oxidation is similar. A small peak is observed for **open-EDOT** during the reduction process which can be associated with the formation of dimeric species.

Open-EDOT and **open-EDTT** show one reversible reduction peak at $E_{1/2}$ = -1.65 and -1.59 V, respectively. This process can be ascribed to the formation of the radical anion in the central core. The higher electron-donating character of the EDOT units in **open-EDOT,** compared to **open-EDTT**, destabilises the formation radical anion and therefore the reduction occurs at more negative potentials.

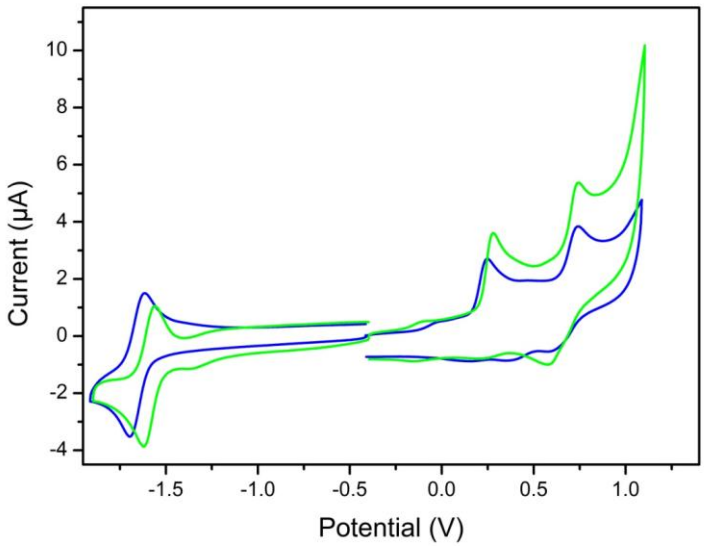

Figure 2.4. Cyclic voltammograms of **open-EDOT** (blue) and **open-EDTT** (green).

The oxidation of the close ring BODIPYs is shown in Figure 2.5. **close-EDOT** shows a first quasi-reversible peak at $E_{1/2}$ = +0.31 V and a second irreversible one at +1.69 V, respectively. The irreversibility in substituted and unsubstituted BODIPY systems has been already described.[37,47] **Close-EDTT** shows only one quasi-reversible peak at $E_{1/2}$ = +0.54 V. At higher potentials **close-EDTT** did not show further oxidation processes before oxidation of the background occurred. Again, the first oxidation peaks can be ascribed to the formation of the radical cation species, whereas the second one, in **close-EDOT**, is associated to the radical dication. As it has been seen for the **open-EDOT**, the close system also shows small peaks when the system is reduced to a neutral state.

Interestingly, the first oxidation potentials for both **close-EDOT** and **close-EDTT** differ significantly. Whereas, in the open systems the oxidation peaks appear at similar values (+0.24 and +0.26 V for **open-EDOT** and **open-EDOT**, respectively), a difference of 0.23 V exits between the close ring BODIPYs. This effect might arise from the existence of non-covalent interactions between the fluorine and the sulfur atoms as it has been seen for similar compounds by computational analysis.[38] In the

case of **close-EDTT**, the S···F interaction can occur between a fluorine of the core and a sulfur bridge atom, and can push the first oxidation towards higher potentials.

Close-EDOT and **close-EDTT** show reversible peaks upon reduction at -1.35 and -1.21 V respectively, associated with the formation of the radical anion. As it has been already reported, the reduction of these compounds relies on the BODIPY core.[37,38] Again, the smaller tendency of the EDTT unit to donate electron-density provokes a higher stabilisation of the radical anion and therefore the reduction occurs at a less negative value. This fact indicates that the EDOT and EDTT units not only determine the behaviour upon oxidation of the monomers, but they also contribute significantly to the reduction processes.

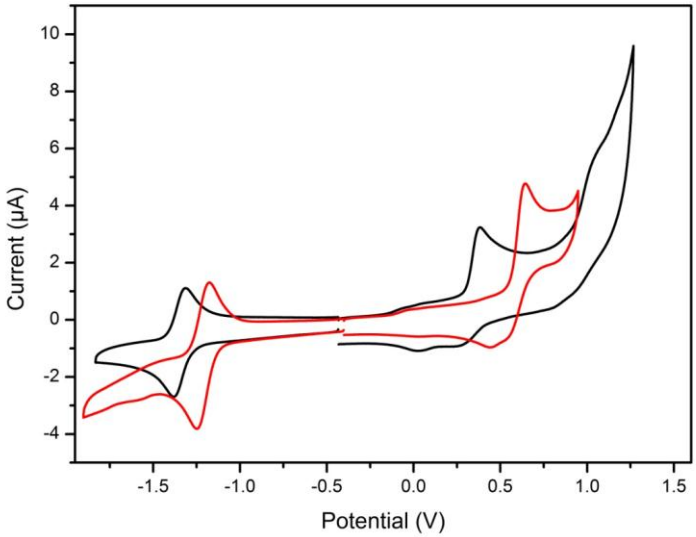

Figure 2.5. Cyclic voltammograms of **close-EDOT** (black) and **close-EDTT** (red).

The HOMO, LUMO levels and HOMO-LUMO gaps of the monomers were calculated from the onset of the first oxidation and reduction processes and referred to ferrocene (-4.8 eV) and they are summarised in Table 2.2. From these results, two general tendencies can be observed**.** Firstly, the open systems have higher HOMO-LUMO gaps than the close rings and secondly, that the EDOT containing monomers

have lower band gaps in comparison to the monomers with EDTT units. It is worth noting that all four monomers show ambipolar behaviour.

	E_{1ox} / V	E_{2ox} / V	E_{1red} / V	HOMO / eV	LUMO / eV	Band Gap / eV
open-EDOT	+0.24 [ir]	+0.74/ +0.60 [r]	-1.70/ -1.61[r]	-4.96	-3.24	1.72
open-EDTT	+0.26 [ir]	+0.75/ +0.59 [q]	-1.62/ -1.56 [r]	-5.04	-3.29	1.75
close-EDOT	+0.38/ +0.25 [r]	+1.69 [q]	-1.38/ -1.32 [r]	-5.10	-3.53	1.57
close-EDTT	+0.63/ +0.45 [q]		-1.24/ -1.18 [r]	-5.32	-3.69	1.63

Table 2.2. Electrochemical data and HOMO-LUMO gaps *open*- and *close*- *Bodipy* derivatives.

2.6 ELECTROPOLYMERISATION OF MONOMERS (13-16) AND ELECTROCHEMICAL PROPERTIES OF THE POLYMERS

To investigate the properties of BODIPY containing polymers, electropolymerisation of monomers **open-EDOT**, **open-EDTT**, **close-EDOT** and **close-EDTT** was carried out in a dichloromethane solution, using tetrabutylammonium hexafluorophosphate ($TBAPF_6$) (0.1M) as the supporting electrolyte with *i*R compensation. The polymers were grown onto a glassy carbon working electrode by repetitive cycling over the first oxidation peak and with a scan rate of 0.1 V/s. The increase of the current over repeated cycles and the development of a new peak at lower potentials due to the higher conjugated system were indicative of polymer growth. The graphs with the electrochemical growth of the polymers are included in this thesis and can be found in the appendix.

Once the electropolymerisations were completed, dark thin films on the surface of the glassy carbon electrode were observed. The redox properties of the polymer were measured by cyclic voltammetry in monomer-free acetonitrile solution using tetrabutylammonium hexafluorophosphate (0.1M) as the supporting electrolyte. All the values are quoted *versus* the redox potential of the ferrocene/ferrocenium couple in acetonitrile. The oxidation and reduction graphs for each compound were obtained independently and not as a full cycle, as the presence of irreversible peaks gave imprecise redox behaviours. Likewise, the solutions were bubbled with argon prior to each reduction.

The electrochemical behaviour of the electrochemically grown polymers is depicted in Figure 2.6 and Table 2.3 summarises all the electrochemical data. All the polymers show only one oxidation process before oxidation of the background occurs. The **p(open-EDOT)**, **p(close-EDOT)** and **p(open-EDTT)** show reversible peaks at +0.29, +0.26 and +0.60 V, respectively. **p(close-EDTT)** shows a quasi-reversible process at +0.74 V.

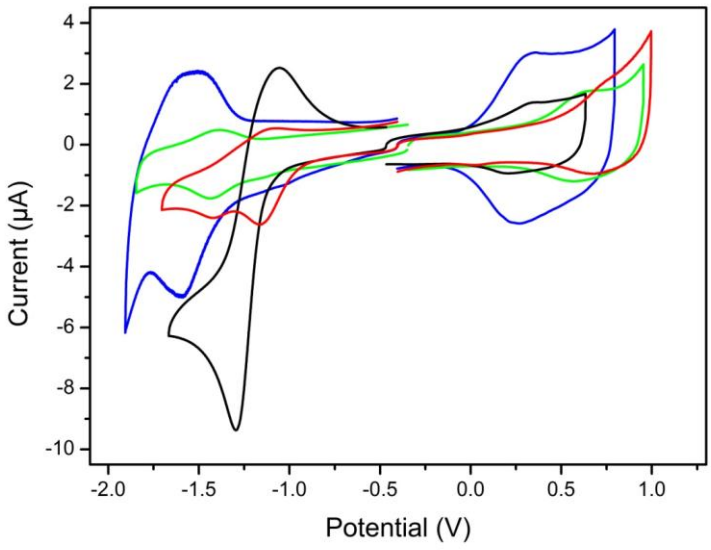

Figure 2.6. Cyclic voltammograms of the electrochemically grown polymers **p(open-EDOT)** (blue), **p(open-EDTT)** (green), **p(close-EDOT)** (black), **p(open-EDTT)** (red).

The reversible reduction of **p(open-EDOT)** appears at -1.55 V. **p(close-EDOT)** and **p(open-EDTT)** show a quasi-reversible peak at -1.19 and -1.40 V, respectively. In the latter reduction, the difference between the anodic and the cathodic peaks is less than 0.59 mV and therefore a two electron process can be occurring. **p(close-EDTT)** shows one quasi-reversible peak at -1.15 V and an irreversible one at -1.43 V.

Whereas the electrochemical properties of the monomers have been compared between open and close rings systems, the electrochemically grown polymers show a very different behaviour. This effect is better understood by studying the onset values of the oxidation and reduction processes, *i.e.* the HOMO and LUMO levels and the band gap of the polymers. These values are summarised in Table 2.3.

	E_{1ox} / V	E_{1red} / V	E_{2red} / V	HOMO / eV	LUMO / eV	Band Gap / eV
p(open-EDOT)	+0.33/ +0.25 [r]	-1.60 /-1.51 [r]		-4.82	-3.44	1.38
p(open-EDTT)	+0.65/ +0.55 [r]	-1.43/ -1.39 [q]		-5.10	-3.60	1.50
p(close-EDOT)	+0.33/ +0.19 [r]	-1.29/ -1.05 [q]		-4.85	-3.66	1.19
p(close-EDTT)	+0.75/ +0.68 [q]	-1.18/ -1.08 [q]	-1.43 [i]	-5.31	-3.86	1.45

Table 2.3. Electrochemical data and band-gaps of electropolymerised *open*- and *close*- *Bodipy* derivatives.

The polymers bearing EDTT units show higher oxidation potentials than those polymers with EDOT units. The HOMO levels for **p(open-EDTT)** and **p(close-EDTT)** are -5.10 and -5.31 eV respectively. By comparison with the HOMO levels of their monomers, these values are almost identical (-5.04 eV for **open-EDTT** and -5.30 eV for **close-EDTT**). Even though the polymer growth is effective (see appendix), the aforementioned F···S interactions and the development of the new

twisted bis-EDTT units along the polymer can impede the alignment of the bis-EDTT units with the BODIPY core.[45] This lack of alignment and the low degree of overlapping of the π orbitals is detrimental for obtaining an effective conjugated system along the polymer, thus explaining the values.

The polymers with EDOT units show low band gaps (1.38 eV for **p(open-EDOT)** and 1.19 eV for **p(close-EDOT)**. This effect might be due to the fact that the new bis-EDOT units that are created remain in a more planar conformation caused by the arising S···O interactions between atoms of adjacent EDOT units. Even though the conjugation system may be disturbed in the EDTT containing polymers, such polymers exhibit small band gaps due to the stabilisation of the LUMO levels, which compared to their EDOT analogues, lie at deeper energy values.

2.7 CHEMICAL SYNTHESIS OF POLYMERS P(BDP-EDOT) AND P(BDP-EDTT) AND THEIR CHARACTERISATION

2.7.1. Polymerisation processes

In order to obtain polymers in bulk to be used in the device fabrication, the close ring containing units polymers were chemically synthesised. At this point different polymerisation approaches were investigated. Some of the polymerisations used in this part of the project have been discussed in the Introduction.

The first polymerisation attempt was carried by oxidative polymerisation of **close-EDTT** using $FeCl_3$ (Sugimoto polymerisation, see Scheme 2.7.). The reaction mechanism of this polymerisation has already been discussed in the Introduction. A solution of the oxidating agent, $FeCl_3$ (4.5 eq), in nitrobenzene was added slowly to a solution of **close-EDTT** in dry chloroform and development of a black precipitate was readily observed. The reaction was stirred at room temperature overnight. The polymerisation process yielded a doped polymer that was treated with hydrazine (2% V:V in methanol) to dedope it and obtain a neutral polymer. In order to remove the

presence of monomers and low molecular weight chains soxhlet extractions were carried out with methanol, acetone and chloroform. The first two fractions were discarded and the black solids obtained from chloroform were studied. Unfortunately, proton nuclear magnetic resonance showed that even though a high degree of polymerisation was obtained, a small peak at around 13 ppm was present (Figure 2.7.b). This peak is attributed to the delocalised proton between two pyrroles units and suggests that partial hydrolysis of the BODIPY ring occurred during the polymerisation. The reason behind is not well understood, although the production of HCl during the reaction can cause the ring opening of the BODIPY core.

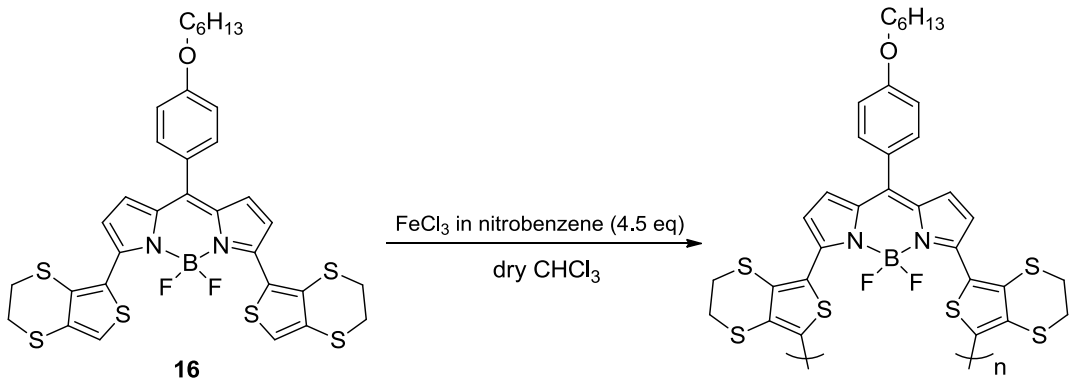

Scheme 2.7. Sugimoto polymerisation of **close-EDTT**

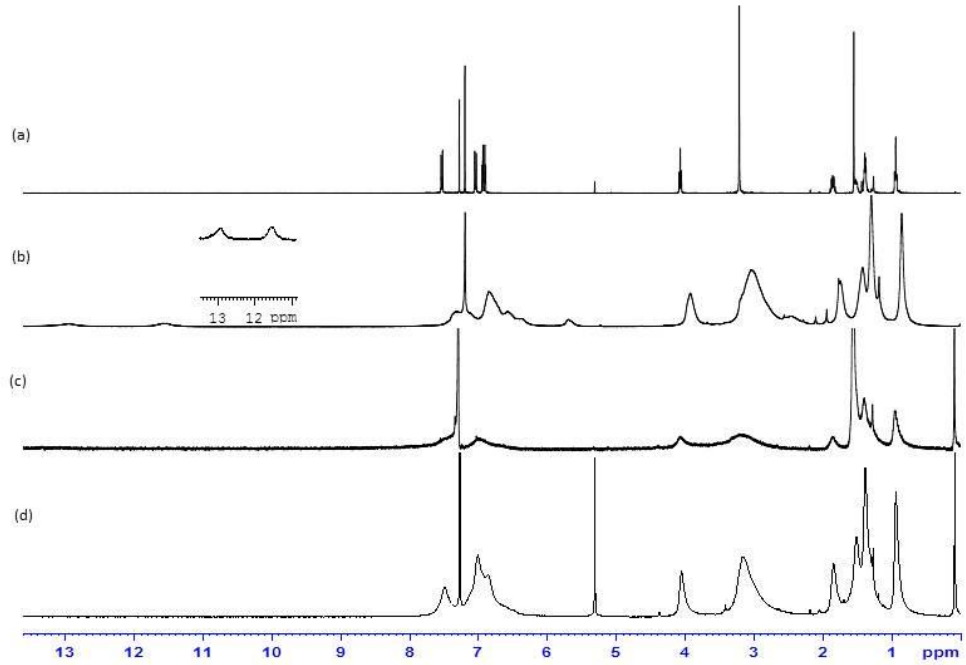

Figure 2.7. H-NMR spectra of **close-EDTT** (a) and **p(close-EDTT)** (Sugimoto (b), polymerisation with nitrosonium cation (c) and Yamamoto (d)).

Due to the opening of the BODIPY ring during the polymerisation with $FeCl_3$, other polymerisations were studied. An oxidative polymerisation using a nitrosonium cation (NO^+) was carried out. The chemistry of the NO^+ cation as a strong oxidating reagent is well-known, having an E^{ox} ~ 1.00 V (in dichloromethane).[48] Although it has not been widely used, nitrosonium containing salts ($NOSbF_6$ and $NOBF_4$) have been employed to polymerise five member-heteroatomic rings such as thiophene, furan, pyrrole and thiazole.[49,50] The reaction mechanism of the polymer-growth is related to other oxidative polymerisations of heteroatomic hydrocarbons. **Close-EDTT** was subjected to polymerisation with one equivalent of nitrosonium tetrafluroborate in dry dichloromethane (in other polymerisations amounts from 10 to 100% of the polymer weight have been used). Due to the instability of the nitrosonium cation (it can readily react with small amounts of water to give NO_2), the

preparation of the reaction was carried out in a glovebox. The reaction was stirred for two days in the dark at room temperature. The aforementioned work-up (precipitation followed by soxhlet extractions) yielded a black polymer. Evidence of no ring opening was observed by proton nuclear magnetic resonance (see figure 2.7.c).

The homopolymerisation of dibrominated aromatic rings can be carried out *via* Yamamoto type reaction. This reaction and its mechanism have been discussed in the Introduction. **Close-EDTT** was brominated twice in the *alpha* positions using 2.1 equivalents of NBS. To a solution of **close-EDTT** in dry dichloromethane (below 0 - ^{o}C and kept in the dark), NBS was slowly added. The reaction was stirred at room temperature overnight and subsequent purification by column chromatography and recrystallization gave compound **32**. Ni(0) mediated homopolymerisation was carried out in DMF by heating the solution at 60 ^{o}C for 48 hours. In this case the polymer is obtained in the neutral state so treatment with a reducing agent is not required. Soxhlet extractions were carried out and the solids obtained from dichloromethane were analysed. As for the previous polymerisation, proton NMR did not show evidence of the opening of the BODIPY ring (see Figure 2.7.d).

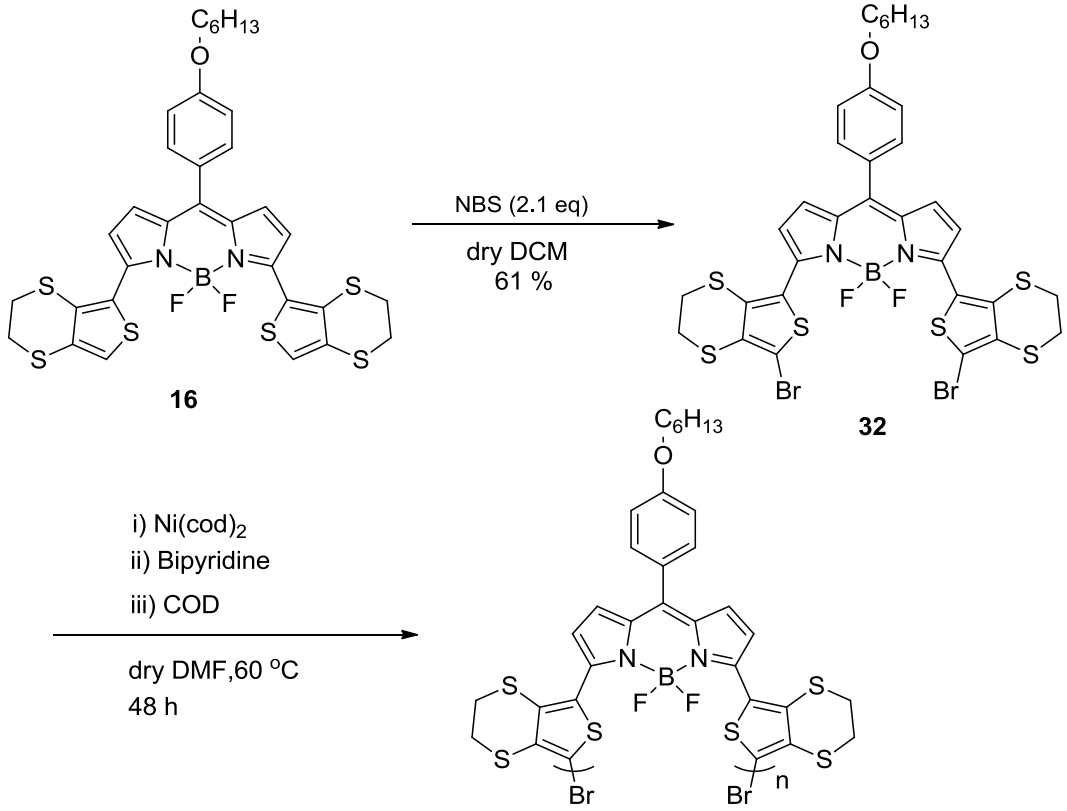

Scheme 2.8. Synthesis of **14** and Yamamoto polymerisation.

The cross coupling reaction between an aromatic system, substituted with halogen atoms (or pseudo-halogen such as the triflate group), and a di-stannylated aromatic derivative *via* Stille coupling has been widely used in the synthesis of conjugated polymers. This reaction has been also discussed in detail in the Introduction. To be able to synthesise polymers in bulk, from relatively easily prepared intermediates, was an attractive feature utilising Stille coupling conditions to obtain the desired conjugated polymers.

The polymers containing the BODIPY core closed were synthesised using this synthetic approach. Scheme 2.9. shows the synthetic route to obtain both the co-monomer and the polymers. The bis-EDTT (**18**) unit was synthesised *via* Ullman coupling from EDTT following a known procedure used for the synthesis of bis-EDOT.[51] Stannylation of bis-EDOT and bis-EDTT gave the two desired co-monomers. Polymerisation of these units with **12** was conducted in the presence of

catalytic amounts of $Pd(PPh_3)_4$. To achieve higher stability, the polymers were end-capped with 2-bromothiophene and stannylated-EDOT or EDTT. The reaction mixture was then poured into methanol to give two black solids. Soxhlet extractions with methanol, acetone, and dichloromethane were carried out to isolate the high molecular weight polymers from the co-monomers and oligomers. In both cases, the solids obtained from the dichloromethane fractions were subjected to full analysis. Likewise, these fractions were used in the fabrication of organic electronic devices (see next section).

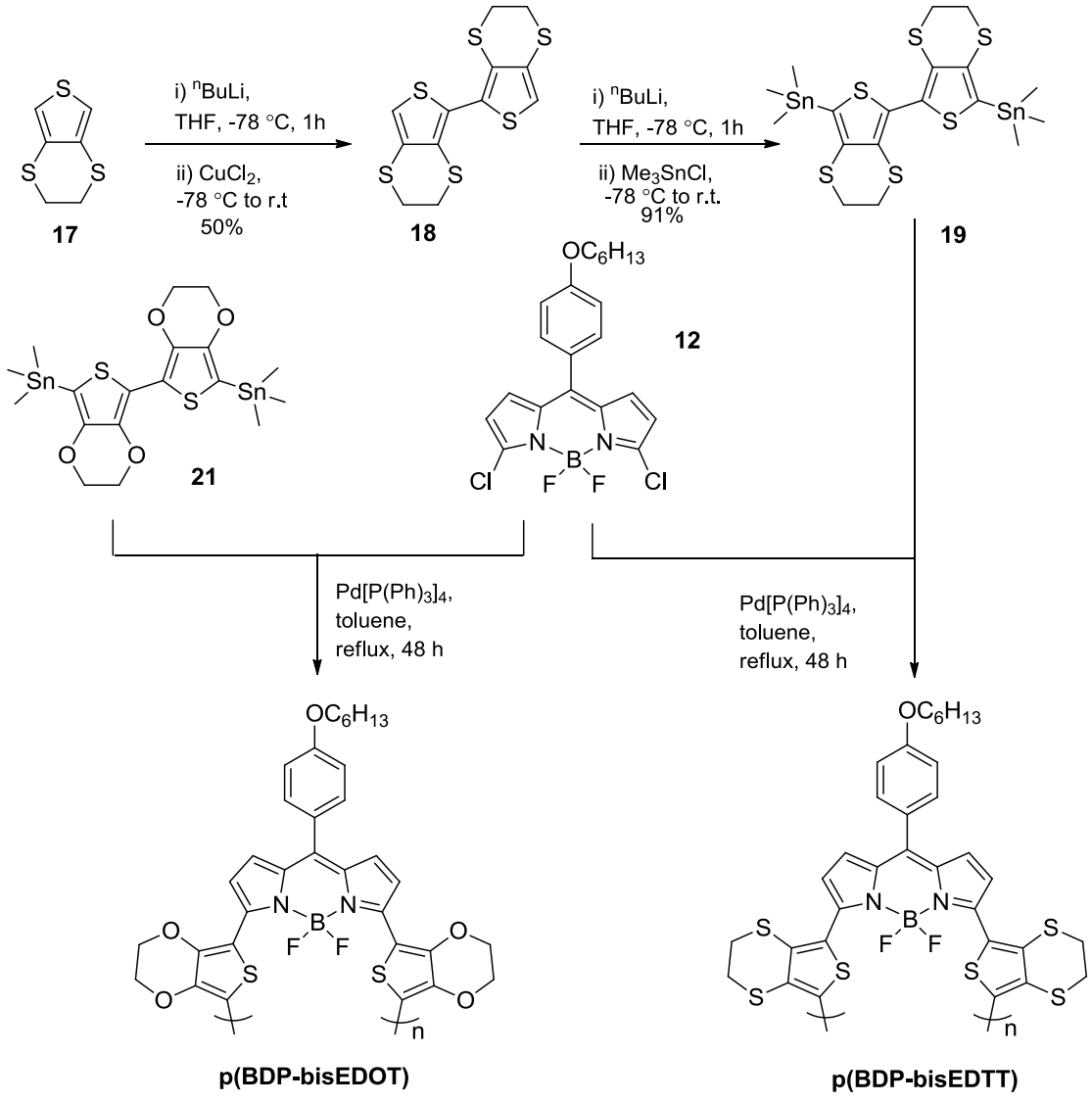

Scheme 2.9. Synthesis of bis-EDTT (**18**), **19** and **p(BDP-bisEDOT)** and **p(BDP-bisEDTT)**.

2.7.2 Characterisation of p(BDP-bisEDOT) and p(BDP-bisEDTT)

The optical properties were characterised by UV-vis spectroscopy (see Table 2.4.). Figure 2.8. shows the UV-visible spectra of copolymers **p(BDP-bisEDOT)** and **p(BDP-bisEDTT)** both in dichloromethane solution and as a film drop-cast on indium tin oxide (ITO). Both copolymers show broad absorption ranges, an important parameter that favours light harvesting for OPVs. Copolymer **p(BDP-bisEDOT)** shows broad absorption from around 300 nm to 1000 nm in solution and up to 1100 nm on thin film. The thin-film of **p(BDP-bisEDOT)** shows a broad absorption peak at 821 nm (*sh* 676 nm) that could be due to the internal charge transfer (ICT) between the bis-EDOT to the BODIPY core. The thin-film spectrum also shows a sharp peak at 426 nm and another one at 569 nm.

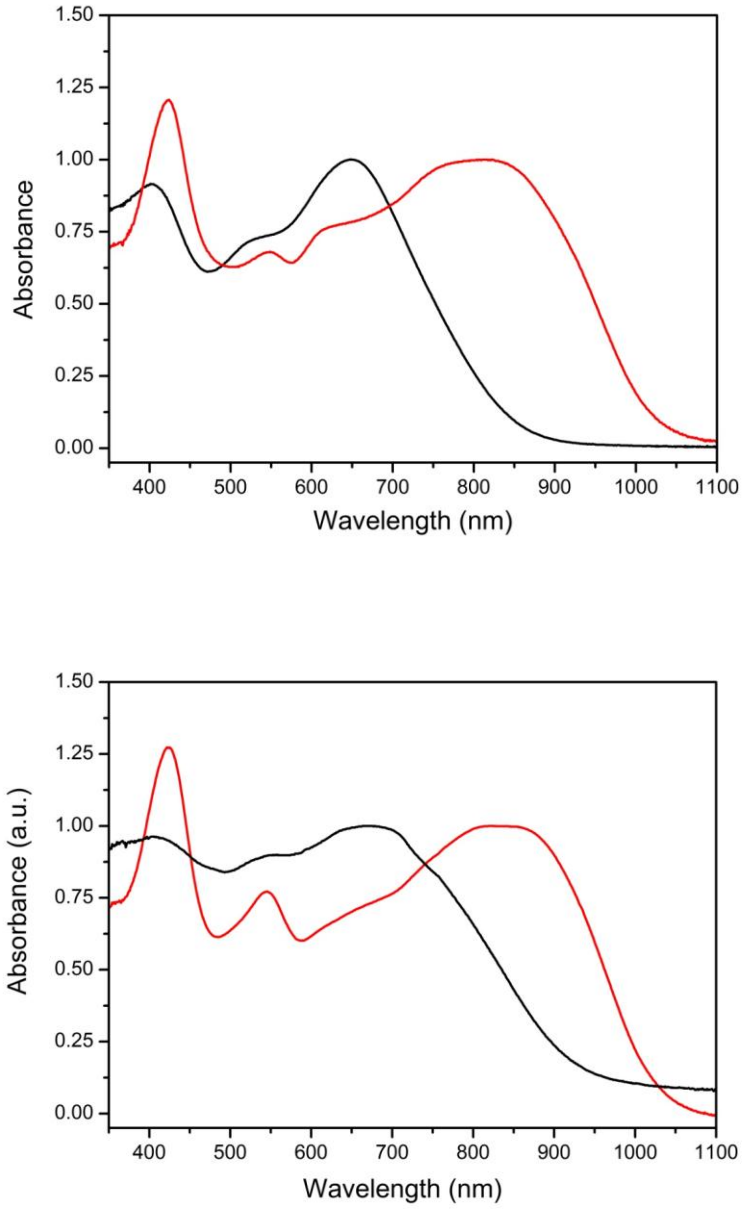

Figure 2.8. UV-visible absorption spectra of **p(BDP-bisEDOT)** (red) and **p(BDP-bisEDTT)** (black) in solution (top) and as a thin-film (bottom).

In the thin-film spectrum of **p(BDP-bisEDTT)** a broad absorption peak at around 669 nm could correspond to ICT. In **p(BDP-bisEDOT)**, the band associated to the ICT is red-shifted 152 nm compared to **p(BDP-bisEDTT)** as the bis-EDOT moiety is a stronger electron donor than bis-EDTT. **p(BDP-bisEDTT)** also shows

absorption at 405 nm and 551 nm (*sh*). Although it is difficult to determine, the optical band gap corresponds to around 1.10 eV for **p(BDP-bisEDOT)** and around 1.35 eV for **p(BDP-bisEDTT)** as the onsets are around 1100 nm and 919 nm, respectively. While the EDTT units in the bis-EDTT are twisted, the more planar spatial configuration of bis-EDOT, due to the favourable O···S interactions between atoms of adjacent EDOT units, results in a higher degree of conjugation, and hence the lower band-gap of **p(BDP-bisEDOT)**.

	UV-vis absortion spectra		$\mathbf{E_{g(film)}}$ **/ eV**
	$\lambda(max)_{sol}$ / nm	$\lambda(max)_{film}$ / nm	
p(BDP-bisEDOT)	818 (br)	821	1.10
p(BDP-bisEDTT)	648	669	1.35

Table 2.4. Optical properties and band-gaps of **p(BDP-bisEDOT)** and **p(BDP-bisEDTT)**.

The electrochemical behavior of the chemically obtained polymers **p(BDP-bisEDOT)** and **p(BDP-bisEDTT)** was determined by cyclic voltammetry analysis with *i*R compensation. The studies were carried out in the solid state by drop-casting a solution of the polymers (in dichloromethane) onto a glassy carbon electrode, which acted as the working electrode. The experiments were carried out at a scan rate of 0.1 V/s. The experiments were carried out in acetonitrile (this solvent does not dissolve the polymers) using tetrabutylammonium hexafluorophosphate (0.1 M) as the supporting electrolyte. All the values are quoted *versus* the redox potential of the ferrocene/ferrocenium couple in acetonitrile. The oxidation and reduction graphs for each compound were obtained independently and not as a full cycle, as the presence of irreversible peaks gave imprecise redox behaviours. Additionally, the solutions were bubbled with argon prior to each reduction process.

Figure 2.9. depicts the oxidation and reduction of polymer **p(BDP-bisEDOT)** and **p(BDP-bisEDTT)**. All the data is summarised in Table 2.5. **p(BDP-bisEDOT)** and **p(BDP-bisEDTT)** show two irreversible oxidations at +0.38 and +0.67 V,

respectively. In accordance with the redox behaviour of the polymers obtained electrochemically, the oxidation potential of the polymer with bis-EDOT units is lower. Equally, both waves show a partially hidden oxidation potential that can be ascribed to the formation of the radical dication. As previously mentioned, the oxidation of this kind of polymer relies on the bis-EDOT or bis-EDTT unit, whereas the reduction relies on the BODIPY core. Although **p(BDP-bisEDTT)** showed an irreversible peak at -1.37 V, the reduction of **p(BDP-bisEDOT)** exhibited some reversibility at -1.38/-1.06 V.

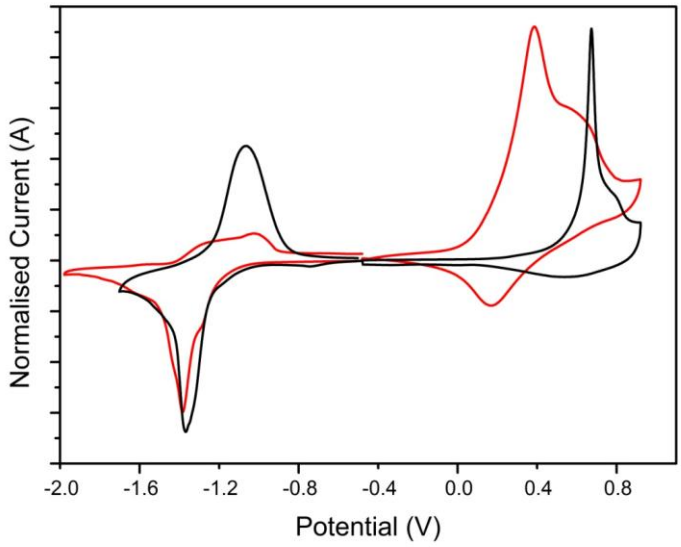

Figure 2.9. Cyclic voltammograms of **p(BDP-bisEDOT)** (red) and **p(BDP-bisEDTT)** (black).

The HOMO and LUMO levels of **p(BDP-bisEDOT)** and **p(BDP-bisEDTT)** were calculated from the onset of the oxidation and reduction waves. The band gaps of the polymers were calculated from the difference of the previously calculated HOMO and LUMO levels (see table 5). The onset of the oxidation of **p(BDP-bisEDOT)** was +0.20 V and of **p(BDP-bisEDTT)** was +0.47 V, giving HOMO levels of -5.00 eV and -5.27 eV respectively. The onsets of the reduction waves for both polymers are similar -1.15 V for **p(BDP-bisEDOT)** and -1.18 V for **p(BDP-bisEDTT)**), giving LUMO levels of -3.65 eV and -3.62 eV.

	E_{1ox} / V	E_{1red} / V	HOMO / eV	LUMO / eV	Band Gap / eV
p(BDP-bisEDOT)	+0.38	-1.37	-5.00	-3.65	1.35
p(BDP-bisEDTT)	+0.67	-1.38/-1.07	-5.27	-3.62	1.65

Table 2.5. Electrochemical and band-gaps of **p(BDP-bisEDOT)** and **p(BDP-bisEDTT)**.

2.8 DEVICE FABRICATION AND CHARACTERISATION

Due to the interesting electronic and electrochemical properties of **p(BDP-bisEDOT)** and **p(BDP-bisEDTT)**, these polymers were tested in organic photovoltaics. All this work has been carried by Calvyn T. Howells and Dr. Salvatore Gambino under the supervision of Professor Ifor D. W. Samuel at the University of St. Andrews.

2.8.1 Photovoltaic Properties of p(BDP-bisEDTT) and p(BDP-bisEDOT)

Two types of device were fabricated, characterised and optimised. The polymer only devices demonstrated low photocurrents; 0.62 $mAcm^{-2}$ and 1.17 $mAcm^{-2}$ for **p(BDP-bisEDTT)** and **p(BDP-bisEDOT)**, respectively (see Figure 2.10). The addition of an electron acceptor, [6,6]-Phenyl-C_{71}-butyric acid methyl ester, dramatically improved performance. A donor acceptor ratio of 1:4 was found to be optimal for both low band-gap polymers. The power conversion efficiency increased from 0.1 to 0.95 % for **p(BDP-bisEDOT)** and from 0.06 % to 0.46 % for **p(BDP-bisEDTT)**, with photocurrents of 7.87 $mAcm^{-2}$ and 4.42 $mAcm^{-2}$, respectively (see Table 2.6.).

Both polymer-fullerene blends demonstrate a broad spectral response (400 nm-1100

nm). For **p(BDP-bisEDOT)** fullerene devices an IPCE of ~ 10, 20, 30 % is observed from 400-600 nm under 0.0, -0.5, -1.0 V bias, respectively. There is a steady decrease in EQE from 600-900 nm. At 900 nm the IPCE under 0.0, -0.5, -1.0 V bias has approximately halved. Between 900-1100 nm we see a sharp fall in EQE. For the **p(BDP-bisEDTT)** fullerene devices, impressive IPCEs are observed between 400-600 nm of >10, 30, 50 % for 0.0, -0.5, -1.0 V bias, repectively. From 600-1100 nm we see a severe fall in IPCE and it is in this region where the **p(BDP-bisEDOT)** fullerene devices outperform the **p(BDP-bisEDTT)** fullerene devices. The large IPCE in the 400-700 nm region can be attributed to the [6,6]-Phenyl-C_{71}-butyric acid methyl ester absorption and its ability to effectively dissociate the exciton allowing, them to contribute to photocurrent (see Figure 2.11.).

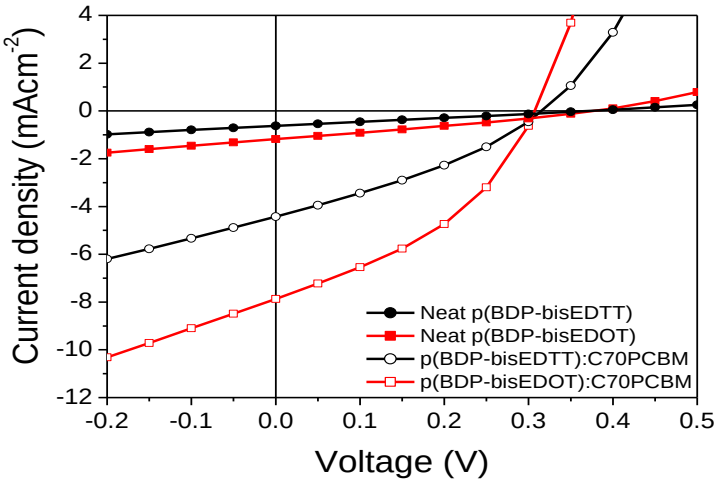

Figure 2.10. J-V characteristics for polymer and polymer-fullerene devices under 100 mW cm^{-2} illumination with standard AM1.5G source.

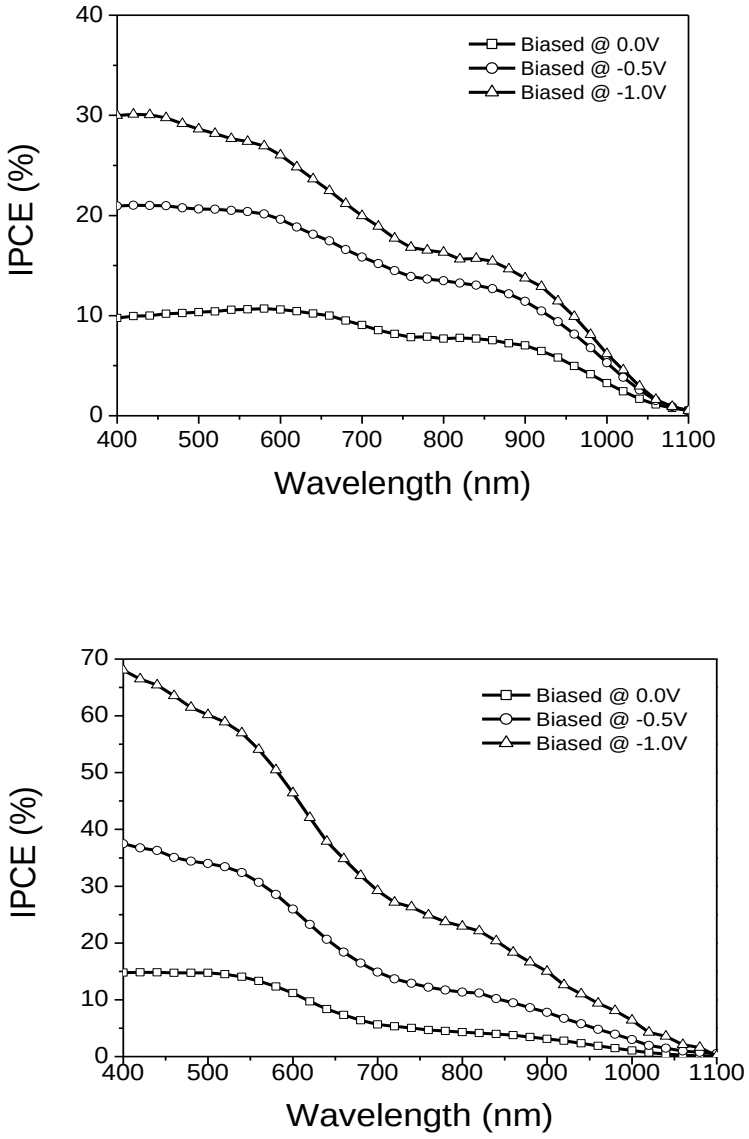

Figure 2.11. Incident photon to electron conversion efficiency (IPCE) for polymer-fullerene devices with and without bias **p(BDP-bisEDOT)** (top) and **p(BDP-bisEDTT)** (bottom).

Active layer	J_{sc} /mAcm^{-2}	V_{oc}/V	FF[%]	PCE[%]
p(BDP-bisEDOT)	1.17	0.31	28	0.10
p(BDP-bisEDTT)	0.62	0.32	30	0.06
p(BDP-bisEDOT):[70]PCBM[a]	7.87	0.37	33	0.95
p(BDP-bisEDTT):[70]PCBM[a]	4.42	0.38	27	0.46

[a] Ratio: Polymer:[70]PCBM (1:4)

Table 2.6. Photovoltaic properties of the **p(BDP-bisEDOT)** and **p(BDP-bisEDTT)**.

2.8.2. Atomic Force Microscopy (AFM) and Time of Flight Measurements of p(BDP-bisEDOT)

The fact that **p(BDP-bisEDOT)** can perform reasonably well without an acceptor led us to think that the polymer could be forming nanostructures by itself. This could explain the dual behaviour of the polymer. In order to investigate the nanostructure of the polymer in the device, a common device was fabricated (ITO/PEDOT:PSS/ **p(BDP-bisEDOT)**) and studied by atomic force microscopy (AFM).

Figure 2.12. shows tapping mode height images of atomic force microscopy (AFM). The image shows the presence of small bead-like structures of **p(BDP-bisEDOT)** spin-coated on ITO/PEDOT substrates**.** The root mean square (rms) roughness was calculated as 42 nm by taking into account a 10 µm x 10 µm scan area that would reflect the actual device under test. While the surface roughness on smoother areas is around 20 nm, the small bead-like structures tend to aggregate and form slightly bigger domains with heights of up to 100 nm. This mixture of aggregate and non-aggregate regions provides a higher average rms roughness of ~42 nm. Smooth bead-like structures are observed on the devices based on ITO/PEDOT/**p(BDP-bisEDOT)**). However, aggregated domains consisting of bigger structures with height of ~100 nm in the **p(BDP-bisEDOT)** coated on the device (ITO/PEDOT/**p(BDP-bisEDOT)**) can be observed as well. This type of aggregation

caused by the wetability of solutions of **p(BDP-bisEDOT)** on different substrates can be improved by optimising thin film fabrication protocols.

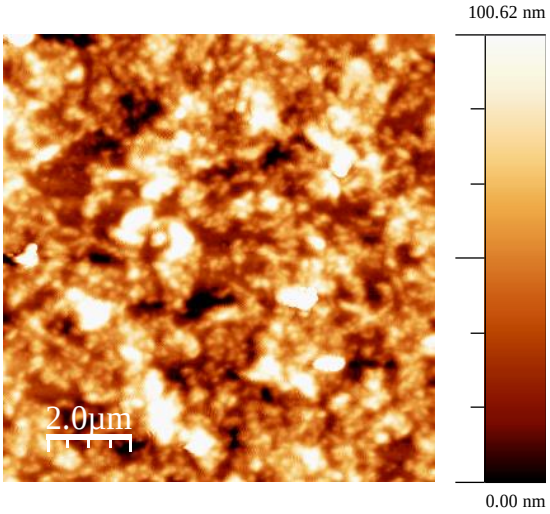

Figure 2.12. Tapping mode AFM height images of **p(BDP-bisEDOT)** on ITO/PEDOT substrate.

The unusual behaviour of **p(BDP-bisEDOT)** in solar cells in the absence of an electron acceptor material that could extract the electrons required further investigation. Therefore, in order to understand this fact, time of flight (TOF) measurements were carried out. Both electron and hole mobilities of **p(BDP-bisEDOT)** were studied. Figure A.8 (Appendix) shows the **p(BDP-bisEDOT)** linear hole photocurrent transient at an electric field of 1.8 x 10^5 Vcm^{-1}. The photocurrent transient shows that the transport is highly dispersive since the linear plot has an exponential like decay instead of a definitive cusp, a plateau and clearly defined knee. However, by plotting the photocurrent transient in a log-log scale figure A.9 (Appendix), a change in the slope was visible. The transit time was determined at each electric field by fitting straight lines before and after the knee as shown in figure A.9 (Appendix). For the above applied electric field the transit time was 39 µs, which corresponds to a mobility value of 1.5 × 10^{-5} cm^2/Vs.

Figure A.10 (Appendix) shows the **p(BDP-bisEDOT)** linear electron photocurrent transient at about 1.8 x 10^5 Vcm^{-1}. Due to the highly dispersive electron photocurrent transient, a log-log scale plot Figure A.11 (Appendix) was studied in order to observe

a significant alteration in the slope of the photocurrent transient. For the above applied electric field the transit time was 7 μs, which corresponds to a mobility value of 7.7×10^{-5} cm^2/Vs.

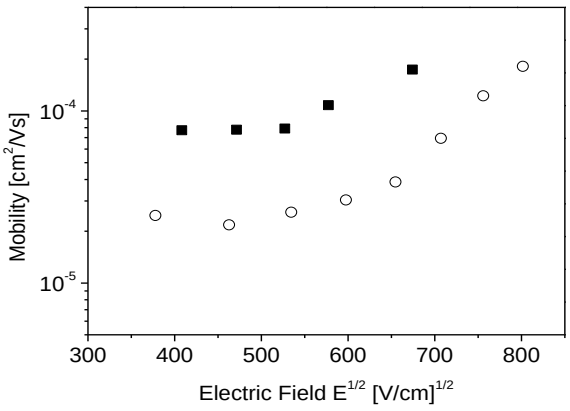

Figure 2.13 Electron (squared dots) and hole (circular dots) mobilities of **p(BDP-bisEDOT)** against the electric field.

TOF mobility measurements were performed in a wide range of electric fields in order to investigate the field dependence of the mobility. Figure 2.13. shows both electron and hole mobility as a function of the square root of the electric field. The most important result is that **p(BDP-bisEDOT)** is an ambipolar charge transport carrier material. In fact both electron and hole mobility values are of the same order of magnitude. Usually for a p-type (n-type) material, electron mobility is orders of magnitude lower than hole mobility, or *vice versa*. However, we can clearly see from Figure 2.13. that electron mobility values are approximately three times higher than hole mobility, indicative of ambipolar behaviour.

Furthermore, Figure 2.13. demonstrates that both carriers show a similar field dependence. It can be clearly seen that at low fields ($E < 3 \times 10^5$ V/cm [$E^{1/2} < 600$ V/cm]) mobility is nearly field independent and its value turned out to be in the range of 2.5 x 10^{-5} cm^2/Vs and 7.5 x 10^{-5} cm^2/Vs, for the holes and the electrons respectively. As the electric field increases further a classic Poole-Frenkel like mobility dependence is shown. Mobility increases nearly an order of magnitude from

3×10^{-5} cm^2 /Vs up to 2×10^{-4} cm^2 /Vs for the holes and from 7×10^{-5} cm^2 /Vs up to 3.2×10^{-4} cm^2 /Vs for the electrons as the as the field increases from 3.5×10^5 V/cm to 6.5×10^5 V/cm.

2.9 CONCLUSIONS AND FURTHER WORK

In conclusion, four new BODIPY derivatives based on a BODIPY core and EDOT or EDTT units have been synthesised. The influence of closing the BODIPY ring (through an N-B-N bridge) or leaving the ring of the dipyrromethene opened was investigated. Likewise, in order to incorporate these monomers into soluble processable conjugated comonomers, a long alkoxy chain was incorporated on the *para*-position of the phenyl ring at the *meso*-position of the BODIPY core.

The four monomers were electropolymerised and the electronic properties were studied by cyclic voltammetry. In order to obtain the polymers in bulk, different polymerisation methods were carried out using **close-EDTT** as the monomer. Sugimoto polymerisation led to the ring opening of the BODIPY core. Another oxidative polymerisation was studied using the nitrosonium ion as the oxidating agent. Equally, Yamamoto polymerisation was carried out using the dibrominated derivative of **close-EDTT** as the monomer.

The best results were obtained *via* Stille coupling polymerisation. The chlorinated BODIPY core was reacted with bis-stannylated-bisEDOT and bis-stannylated-bisEDTT and two low band-gap copolymers (**p(BDP-bisEDOT)** and **p(BDP-bisEDTT)**) were obtained in good yields. These polymers were fully characterised and used in device fabrication.

The photovoltaic properties of both copolymers were investigated. **p(BDP-bisEDOT)** and **p(BDP-bisEDTT)** showed a power conversion efficiency of 0.95 and 0.46%, respectively. Interestingly, the devices fabricated from neat **p(BDP-bisEDOT)** showed an efficiency as high as 0.1%. In order to investigate the reason for this value, time-of-flight studies were carried out. Unlike most of the organic semiconductors, which show remarkable differences between the hole and electron mobility, **p(BDP-bisEDOT)** shows well balanced mobilities, indicating ambipolar behaviour.

The incorporation of the BODIPY core into conjugated polymers and their use in OPVs has been proved with these two polymers. However, the poor V_{OC} of the devices when the polymers are blended with different acceptors impedes a higher performance. Likewise, during the processing of the devices, the polymers showed limited solubility in common solvents, leading to poor film qualities.

In order to overcome these problems, optimisation of the chemical structure of the polymers should be completed. This includes the incorporation of donor moieties with lower HOMO levels that can lead to an increase in the V_{OC}. The BODIPY core can therefore be co-polymerised with, for example, carbazoles or fluorenes which apart from showing a lower HOMO level, can give higher solubility to the co-polymer due to the alkyl chains present in these units.

REFERENCES

1. A. Loudet and K. Burgess, *Chemical Reviews*, 2007, **107**, 4891-4932.
2. G. Ulrich, R. Ziessel and A. Harriman, *Angewandte Chemie International Edition*, 2008, **47**, 1184-1201.
3. N. Boens, V. Leen and W. Dehaen, *Chemical Society Reviews*, 2012, **41**, 1130-1172.
4. A. C. Benniston and G. Copley, *Physical Chemistry Chemical Physics*, 2009, **11**, 4124-4131.
5. L. Bonardi, H. Kanaan, F. Camerel, P. Jolinat, P. Retailleau and R. Ziessel, *Advanced Functional Materials*, 2008, **18**, 401-413.
6. R. Y. Lai and A. J. Bard, *The Journal of Physical Chemistry B*, 2003, **107**, 5036-5042.
7. A. B. Nepomnyashchii, M. Bröring, J. Ahrens and A. J. Bard, *Journal of the American Chemical Society*, 2011, **133**, 8633-8645.
8. T. L. Arbeloa, F. L. Arbeloa, I. L. Arbeloa, I. García-Moreno, A. Costela, R. Sastre and F. Amat-Guerri, *Chemical Physics Letters*, 1999, **299**, 315-321.
9. O. García, L. Garrido, R. Sastre, A. Costela and I. García-Moreno, *Advanced Functional Materials*, 2008, **18**, 2017-2025.
10. M. A. H. Alamiry, A. C. Benniston, G. Copley, K. J. Elliott, A. Harriman, B. Stewart and Y.-G. Zhi, *Chemistry of Materials*, 2008, **20**, 4024-4032.
11. O. A. Bozdemir, R. Guliyev, O. Buyukcakir, S. Selcuk, S. Kolemen, G. Gulseren, T. Nalbantoglu, H. Boyaci and E. U. Akkaya, *Journal of the American Chemical Society*, 2010, **132**, 8029-8036.
12. S. Kolemen, O. A. Bozdemir, Y. Cakmak, G. Barin, S. Erten-Ela, M. Marszalek, J.-H. Yum, S. M. Zakeeruddin, M. K. Nazeeruddin, M. Gratzel and E. U. Akkaya, *Chemical Science*, 2011, **2**, 949-954.
13. S. Erten-Ela, M. D. Yilmaz, B. Icli, Y. Dede, S. Icli and E. U. Akkaya, *Organic Letters*, 2008, **10**, 3299-3302.
14. B. Kim, B. Ma, V. R. Donuru, H. Liu and J. M. J. Frechet, *Chemical Communications*, 2010, **46**, 4148-4150.

15. A. Treibs and F.-H. Kreuzer, *Justus Liebigs Annalen der Chemie*, 1968, **718**, 208-223.
16. I. J. Arroyo, R. Hu, G. Merino, B. Z. Tang and E. Peña-Cabrera, *The Journal of Organic Chemistry*, 2009, **74**, 5719-5722.
17. D. T. Gryko, D. Gryko and C.-H. Lee, *Chemical Society Reviews*, 2012, **41**, 3780-3789.
18. V. Leen, V. Z. Gonzalvo, W. M. Deborggraeve, N. Boens and W. Dehaen, *Chemical Communications*, 2010, **46**, 4908-4910.
19. Z. Dost, S. Atilgan and E. U. Akkaya, *Tetrahedron*, 2006, **62**, 8484-8488.
20. E. Deniz, G. C. Isbasar, O. A. Bozdemir, L. T. Yildirim, A. Siemiarczuk and E. U. Akkaya, *Organic Letters*, 2008, **10**, 3401-3403.
21. M. Baruah, W. Qin, R. A. L. Vallée, D. Beljonne, T. Rohand, W. Dehaen and N. Boens, *Organic Letters*, 2005, **7**, 4377-4380.
22. T. Rohand, W. Qin, N. Boens and W. Dehaen, *European Journal of Organic Chemistry*, 2006, **2006**, 4658-4663.
23. J. Han, O. Gonzalez, A. Aguilar-Aguilar, E. Pena-Cabrera and K. Burgess, *Organic & Biomolecular Chemistry*, 2009, **7**, 34-36.
24. C. Kusturin, L. S. Liebeskind, H. Rahman, K. Sample, B. Schweitzer, J. Srogl and W. L. Neumann, *Organic Letters*, 2003, **5**, 4349-4352.
25. J.-s. Lu, H. Fu, Y. Zhang, Z. J. Jakubek, Y. Tao and S. Wang, *Angewandte Chemie International Edition*, 2011, **50**, 11658-11662.
26. O. Altan Bozdemir, S. Erbas-Cakmak, O. O. Ekiz, A. Dana and E. U. Akkaya, *Angewandte Chemie International Edition*, 2011, **50**, 10907-10912.
27. A. Nagai, J. Miyake, K. Kokado, Y. Nagata and Y. Chujo, *Journal of the American Chemical Society*, 2008, **130**, 15276-15278.
28. A. Nagai, K. Kokado, J. Miyake and Y. Cyujo, *Journal of Polymer Science Part A: Polymer Chemistry*, 2010, **48**, 627-634.
29. R. París, I. Quijada-Garrido, O. García and M. Liras, *Macromolecules*, 2010, **44**, 80-86.
30. P. Hewavitharanage, P. Nzeata and J. Wiggins, *Synthesis of an E-BODIPY based fluorescent Co-polymer containing organoboron quinolate units*, 2012.

31. V. R. Donuru, G. K. Vegesna, S. Velayudham, G. Meng and H. Liu, *Journal of Polymer Science Part A: Polymer Chemistry*, 2009, **47**, 5354-5366.
32. F. E. Alemdaroglu, S. C. Alexander, D. Ji, D. K. Prusty, M. Börsch and A. Herrmann, *Macromolecules*, 2009, **42**, 6529-6536.
33. B. C. Popere, A. M. Della Pelle and S. Thayumanavan, *Macromolecules*, 2011, **44**, 4767-4776.
34. S. Zhu, N. Dorh, J. Zhang, G. Vegesna, H. Li, F.-T. Luo, A. Tiwari and H. Liu, *Journal of Materials Chemistry*, 2012, **22**, 2781-2790.
35. P. Camurlu, C. Gültekin and Z. Bicil, *Electrochimica Acta*, 2012, **61**, 50-56.
36. A. Cihaner and F. Algı, *Reactive and Functional Polymers*, 2009, **69**, 62-67.
37. F. Algı and A. Cihaner, *Organic Electronics*, 2009, **10**, 453-458.
38. J. C. Forgie, P. J. Skabara, I. Stibor, F. Vilela and Z. Vobecka, *Chemistry of Materials*, 2009, **21**, 1784-1786.
39. E. D. T. Rohand, T. H. Ngo, W. Maes, and Wim Dehaen *Arkivoc*, 2007, **X**, 307-324.
40. L. Li, J. Han, B. Nguyen and K. Burgess, *The Journal of Organic Chemistry*, 2008, **73**, 1963-1970.
41. L. Groenendaal, G. Zotti, P. H. Aubert, S. M. Waybright and J. R. Reynolds, *Advanced Materials*, 2003, **15**, 855-879.
42. *Handbook of Chalcogen Chemistry. New Perspectives in Sulfur, Selenium and Tellurium.*, Royal Society of Chemistry, Cambridge, 2007.
43. H. Pang, P. J. Skabara, S. Gordeyev, J. J. W. McDouall, S. J. Coles and M. B. Hursthouse, *Chemistry of Materials*, 2006, **19**, 301-307.
44. C. Wang, J. L. Schindler, C. R. Kannewurf and M. G. Kanatzidis, *Chemistry of Materials*, 1995, **7**, 58-68.
45. H. J. Spencer, P. J. Skabara, M. Giles, I. McCulloch, S. J. Coles and M. B. Hursthouse, *Journal of Materials Chemistry*, 2005, **15**, 4783-4792.
46. C. O. Kappe, *Angewandte Chemie International Edition*, 2004, **43**, 6250-6284.
47. A. B. Nepomnyashchii, S. Cho, P. J. Rossky and A. J. Bard, *Journal of the American Chemical Society*, 2010, **132**, 17550-17559.

48. N. G. Connelly and W. E. Geiger, *Chemical Reviews*, 1996, **96**, 877-910.
49. G. Koßmehl and G. Chatzitheodorou, *Die Makromolekulare Chemie, Rapid Communications*, 1983, **4**, 639-643.
50. G. Koßmehl, *Makromolekulare Chemie. Macromolecular Symposia*, 1986, **4**, 45-64.
51. J. Roncali, P. Blanchard and P. Frere, *Journal of Materials Chemistry*, 2005, **15**, 1589-1610.